jove

Temperature-Controlled Assembly and Characterization of a Droplet Interface Bilayer

Jessie D. Ringley[1], **Stephen Andrew Sarles**[1]

[1] Department of Mechanical, Aerospace and Biomedical Engineering, University of Tennessee

Corresponding Author

Stephen Andrew Sarles
ssarles@utk.edu

Citation

Ringley, J.D., Sarles, S.A. Temperature-Controlled Assembly and Characterization of a Droplet Interface Bilayer. *J. Vis. Exp.* (170), e62362, doi:10.3791/62362 (2021).

Date Published

April 19, 2021

DOI

10.3791/62362

URL

jove.com/video/62362

Abstract

The droplet interface bilayer (DIB) method for assembling lipid bilayers (i.e., DIBs) between lipid-coated aqueous droplets in oil offers key benefits versus other methods: DIBs are stable and often long-lasting, bilayer area can be reversibly tuned, leaflet asymmetry is readily controlled via droplet compositions, and tissue-like networks of bilayers can be obtained by adjoining many droplets. Forming DIBs requires spontaneous assembly of lipids into high density lipid monolayers at the surfaces of the droplets. While this occurs readily at room temperature for common synthetic lipids, a sufficient monolayer or stable bilayer fails to form at similar conditions for lipids with melting points above room temperature, including some cellular lipid extracts. This behavior has likely limited the compositions—and perhaps the biological relevance—of DIBs in model membrane studies. To address this problem, an experimental protocol is presented to carefully heat the oil reservoir hosting DIB droplets and characterize the effects of temperature on the lipid membrane. Specifically, this protocol shows how to use a thermally conductive aluminum fixture and resistive heating elements controlled by a feedback loop to prescribe elevated temperatures, which improves monolayer assembly and bilayer formation for a wider set of lipid types. Structural characteristics of the membrane, as well as the thermotropic phase transitions of the lipids comprising the bilayer, are quantified by measuring the changes in electrical capacitance of the DIB. Together, this procedure can aid in evaluating biophysical phenomena in model membranes over various temperatures, including determining an effective melting temperature (T_M) for multi-component lipid mixtures. This capability will thus allow for closer replication of natural phase transitions in model membranes and encourage the formation and use of model membranes from a wider swath of membrane constituents, including those that better capture the heterogeneity of their cellular counterparts.

Introduction

Cellular membranes are selectively permeable barriers comprised of thousands of lipid types[1], proteins, carbohydrates, and sterols that encapsulate and subdivide all living cells. Understanding how their compositions affect their functions and revealing how natural and synthetic molecules interact with, adhere to, disrupt, and translocate cellular membranes are, therefore, important areas of research with wide-reaching implications in biology, medicine, chemistry, physics, and materials engineering.

These aims for discovery directly benefit from proven techniques for assembling, manipulating, and studying model membranes—including lipid bilayers assembled from synthetic or naturally occurring lipids—that mimic the composition, structure, and transport properties of their cellular counterparts. In recent years, the droplet interface bilayer (DIB) method[2,3,4] for constructing a planar lipid bilayer between lipid-coated water droplets in oil has received significant attention[5,6,7,8,9,10,11,12,13,14,15,16,17,18,19,20,21,22,23], and has demonstrated practical advantages over other approaches for model membrane formation: the DIB method is simple to perform, requires no sophisticated fabrication or preparation (e.g., "painting") of a substrate to support the membrane, consistently yields membranes with superior longevity, allows for standard electrophysiology measurements, and simplifies the formation of model membranes with asymmetric leaflet compositions[3]. Because the bilayer forms spontaneously between droplets and each droplet can be tailored in position and makeup, the DIB technique has also attracted considerable interest in developing cell-inspired material systems that build on the use of stimuli-responsive membranes[18,24,25,26,27,28,29], balanced compartmentalization and transport[14,30,31], and tissue-like materials[17,23,32,33,34,35,36].

The majority of published experiments on model membranes, including those with DIBs, have been performed at room temperature (RT, ~20-25 °C) and with a handful of synthetic lipids (e.g., DOPC, DPhPC, etc.). This practice limits the scope of biophysical questions that can be studied in model membranes and, based on observation, it can also restrict the types of lipids that can be used to assemble DIBs. For example, a synthetic lipid such as DPPC, which has a melting temperature of 42 °C, does not assemble tightly-packed monolayers or form DIBs at RT[37]. DIB formation at room temperature has also proven difficult for natural extracts, such as those from mammals (e.g., brain total lipid extract, BTLE)[38] or bacteria (e.g., *Escherichia coli* total lipid extract, ETLE)[37], which contain many different types of lipids and originate from cells that reside at elevated temperatures (37 °C). Enabling study of diverse compositions thus provides opportunities to understand membrane-mediated processes in biologically relevant conditions.

Raising the temperature of the oil can serve two purposes: it increases the kinetics of monolayer assembly and it can cause lipids to undergo a melting transition to reach a liquid disordered phase. Both consequences aid in monolayer assembly[39], a pre-requisite for a DIB. In addition to heating for bilayer formation, cooling the membrane after the formation can be used to identify thermotropic transitions in single lipid bilayers[38], including those in natural lipid mixtures (e.g., BTLE) that can be difficult to detect using calorimetry. Aside from assessing thermotropic transitions of lipids, precisely varying the temperature of the DIB

can be used to study temperature-induced changes in membrane structure[38] and examine how lipid composition and fluidity affect the kinetics of membrane-active species (e.g., pore-forming peptides and transmembrane proteins[37]), including mammalian and bacterial model membranes at a physiologically relevant temperature (37 °C).

Herein, a description of how to assemble a modified DIB oil reservoir and operate a feedback-temperature controller to enable monolayer assembly and bilayer formation at temperatures higher than RT will be explained. Distinguished from a previous protocol[40], explicit detail is included regarding the integration of instrumentation needed for measuring and controlling temperature in parallel to assembly and characterization of the DIB in the oil reservoir. The procedure will thus enable a user to apply this method for forming and studying DIBs across a range of temperatures in a variety of scientific contexts. Moreover, the representative results provide specific examples for the types of measurable changes in both membrane structure and ion transport that can occur as temperature is varied. These techniques are important additions to the many biophysical studies that can be designed and performed effectively in DIBs, including studying the kinetics of membrane-active species in different membrane compositions.

Protocol

1. Heated fixture preparation

1. Gather 2 pieces of 1 mm thick insulative rubber trimmed to 25 mm x 40 mm in width and length, respectively, 2 pieces of a 6 mm-thick rubber that are also 25 mm x 40 mm, a prepared aluminum base fixture assembly, and an acrylic oil reservoir that fits in the viewing window of the aluminum base fixture (see **Figures S1, S2, and S3** for details on fabrication and an exploded view of assembly). Prepare the aluminum fixture first by attaching to the bottom of the fixture a glass coverslip viewing window with UV curable adhesive and adhering 1 resistive heating element to the top of each 25 mm x 25 mm side flange of the fixture.
2. Place the thinner rubber pieces onto the stage of the microscope such that the long edge of each piece is tangential to the stage opening as shown in (**Figure 1**).
3. Position the aluminum-base fixture on top of the insulative pads with the viewing window of the fixture centered above the objective lens. Proper alignment is required for imaging the connected droplets.
4. Place a thicker piece of rubber on top of each resistive heating element and use a microscope stage clip to hold it in place. These pieces protect the heating elements from damage caused by the stage clips and insulate against accidental electrical shorting between the heating elements and both the aluminum fixture and the microscope stage.
5. Carefully bend the measurement-end of a thermocouple to achieve a 90° angle at ~4 mm from the end.
6. Insert the bent tip of the thermocouple into the lower left corner of the aluminum fixture and gently secure it with the locking screw.
7. Place the acrylic reservoir into the well of the aluminum fixture. This is done prior to adding hexadecane oil to the well (step 1.8) of the aluminum fixture to minimize the risk of trapping air bubbles between the viewing window and the bottom of the acrylic reservoir, which can obstruct the view of the droplets.
   NOTE: Oil added to the viewing compartment of the aluminum fixture is used to match the refractive indices

of the acrylic and glass for clearer imaging of the droplets contained within the acrylic reservoir. Thus, it is worth noting that oil in the well of the aluminum fixture does not contact the contents of the acrylic reservoir and rigorous cleaning of the aluminum fixture is not required.

8. Dispense ~1,000 µL of hexadecane oil into the well of aluminum fixture (i.e., between the walls of the acrylic reservoir and aluminum fixture), taking care to not overfill. The oil level in the well of the aluminum fixture should be as high as allowable to maximize surface area for heat transfer, while not allowing oil to spill over the edges of the fixture onto the microscope stage or objective lens.

9. Dispense ~1,000 µL of hexadecane oil into the acrylic reservoir, while remaining mindful to not overfill.
NOTE: The acrylic reservoir should always be thoroughly cleaned between experiments. The user must employ a regiment consisting of successive rinses with ethyl-alcohol and deionized water followed by drying in a desiccator bowl for over 12 h.

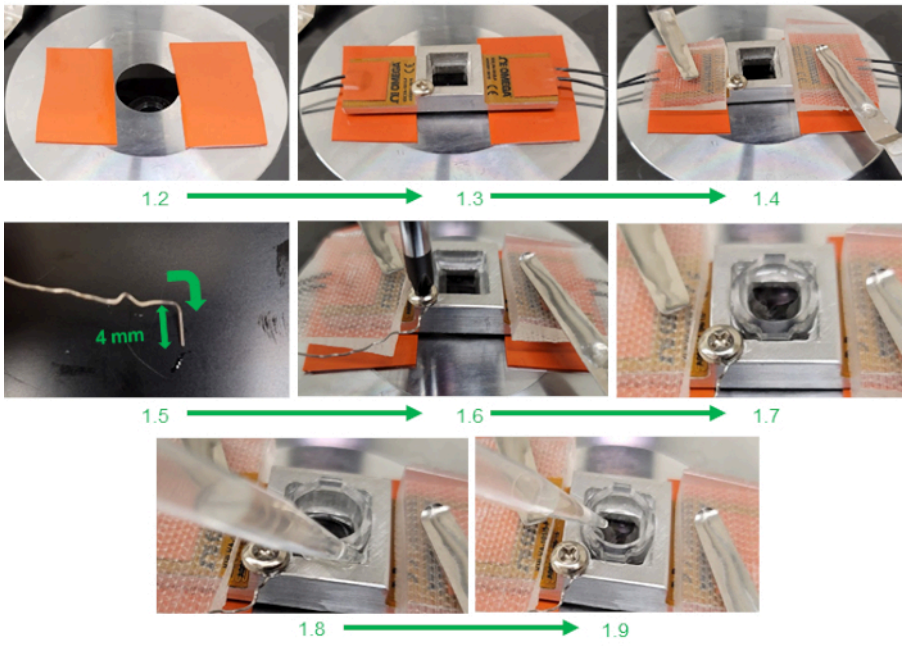

Figure 1: Heated stage assembly. Images show the assembly of the thermally conductive fixture and oil reservoir for DIB formation; numbers beneath each image identify the corresponding step of the protocol. Please click here to view a larger version of this figure.

2. Instrumentation for simultaneous feedback temperature control and electrical characterization of a DIB

NOTE: This protocol integrates the following instruments for enabling feedback temperature control and simultaneous electrical characterization of a DIB: a personal computer (PC) with two available universal serial bus (USB) connections, a patch clamp amplifier paired to a dedicated data acquisition (DAQ-1) system, a waveform generator, a second programable DAQ (DAQ-2) with voltage output and temperature input modules, and a power supply/amplifier. The following steps describe the necessary connections of these instruments (as illustrated in **Figure 2a**) needed for isolating the measurement and control of temperature from simultaneous electrophysiology of a DIB. Substitutions for equivalent instruments may be made as required.

1. Establish output and input connections to the DAQ-2 modules.
    1. Select two pairs of screw terminals on the voltage output module for differential voltage connections and attach wire leads to these locations. Odd number terminals are common ground connections, and the even number terminals are ungrounded outputs, as shown in (**Figure 2c**). Connect each of these two pairs of lead wires to separate screw-terminal-BNC adapters and then connect each adapter to a separate BNC cable used to route voltage signals to other instruments.

        NOTE: In this setup, differential connections at terminals 0 and 1 are assigned for the temperature control output to the power amplifier, while another pair of connections at terminals 6 and 7 are designated for voltage output to be sent to the droplets via the patch clamp amplifier.
    2. Referring to (**Figure 2c**), select one set of thermocouple terminals (e.g., terminals 2 and 3 are designated as the TC1 pair) on the thermocouple input module and connect to it the thermocouple wires.

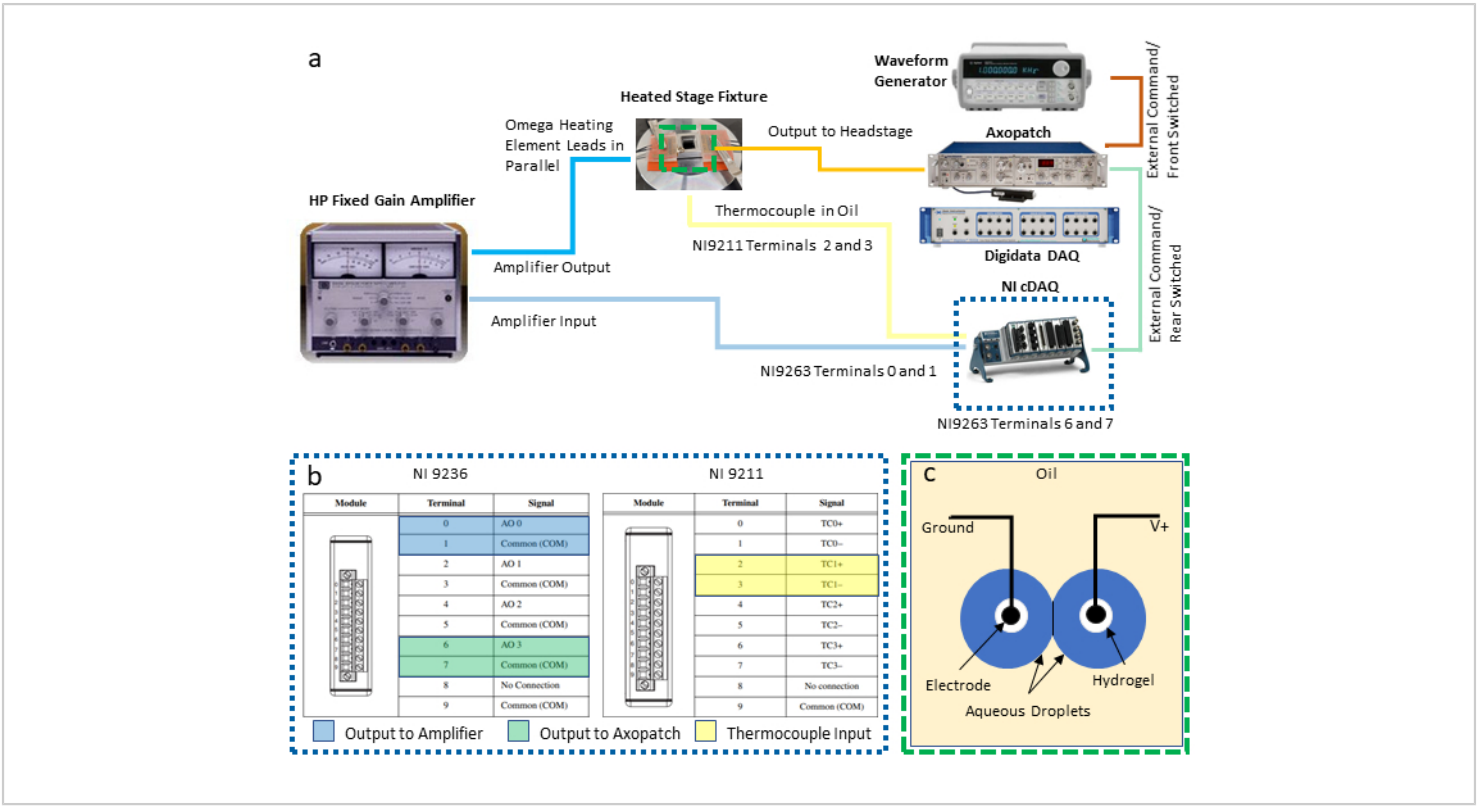

Figure 2: System wiring connections. A schematic of the devices and wiring required for the system is shown in (**a**), while a detailed look at the DAQ-2 connections is provided in (**b**). The illustration in (**c**) shows aqueous droplets on hydrogel-coated electrodes submerged in oil for DIB formation. The two electrodes are connected to the grounded and ungrounded (V +) connections, respectively, on the headstage unit of the patch clamp amplifier. Please click here to view a larger version of this figure.

2. After electrical connections to the DAQ-2 modules have been made, connect the DAQ-2 chassis to a PC via a USB connection and connect to an electrical power source. Then confirm successful driver and software installation prior to use with a commercial software.

3. Configure and connect a power amplifier between DAQ-2 and resistive heating elements.

    1. Configure the amplifier to operate in fixed-gain amplification mode with a gain of 10X.

    2. Using a banana jack-BNC adapter, connect the BNC cable originating from terminals 0 and 1 on the voltage output module (**Figure 2b**) to the input connections on the power amplifier.

    3. Using additional BNC adapters and cabling, connect the output terminals of the power amplifier to both sets of heating elements, which are wired in parallel to one another and the amplifier to ensure that both elements maintain the same voltage drop during use.

4. Establish necessary connections for the electrophysiology equipment.

1. Connect a BNC cable originating from terminals 6 and 7 on the voltage output module (**Figure 2b**) to the Rear Switched External Command BNC connectors on the rear of the patch clamp amplifier.

2. Connect a second BNC cable between the output of waveform generator and the Front Switch External Command connection on the rear of the patch clamp amplifier.

   NOTE: These two connections provide alternative methods for generating voltage waveforms that are applied to the droplet electrodes via the patch clamp amplifier. The waveform generator is especially useful for generating triangular waveform voltages used to measure membrane capacitance. The user may decide which, if either, are necessary for their own application.

3. With a third BNC cable, connect the output of the measured current located on the front panel of the patch clamp amplifier to an available analog input BNC connector on the front of DAQ-1.

4. With a fourth BNC cable, connect the output of measured membrane voltage (on the rear of the patch clamp amplifier) to a separate analog input connector on DAQ-1. This enables digitization of the voltage applied across the electrodes.

5. With the two droplet electrodes prepared and supported on micromanipulators as described in Steps 7-9 in ref.[40], connect the electrode leads to the patch clamp headstage, which is the attached via cable to the patch clamp amplifier.

   NOTE: The role of the headstage is to control the voltage between the electrodes and measure the resulting current, which is converted into a proportional voltage that gets output by the patch clamp amplifier to DAQ-1.

6. Connect DAQ-1 to a PC via a USB connection and connect the corresponding power supply cables to both the patch clamp amplifier and DAQ-1.

5. Power on all measurement equipment.

   NOTE: Perhaps the most important detail in this setup is to ensure the power amplifier output (mA-A) connections are electrically isolated from the headstage unit of the patch clamp amplifier, which uses a sensitive circuit to measure pA-nA level currents in a DIB.

3. Feedback temperature control of droplet interface bilayers

NOTE: The following steps for operating the feedback temperature control system are based on a custom graphical user interface (GUI) created for implementing proportional-integral (PI) feedback temperature control[40,41] (see **Supplementary Coding Files**). Other software and control algorithms may be used instead. A copy of this program is provided to the reader with the supplementary information for the paper, however the user is responsible to configure it for their own equipment and needs.

1. Start the DAQ-2 software on the PC and open the temperature control program file. Once the GUI opens, open the program again by clicking on the folder icon in the bottom left corner of the GUI and selecting the temperature control program (**Figure 3**).

2. Enter appropriate numerical values for the proportional control gain (K_P) and integral control gain (K_I).

   NOTE: K_P and K_I values of 0.598 and 0.00445, respectively, were found to work well in the setup. These values were determined iteratively through

simulation using a system model that incorporates parameters obtained from measured open-loop heating responses (see **Figure 4**). During *open-loop heating*, the prescribed heating power is independent of the measured temperature. In contrast, *closed-loop heating* consists of continually adjusting the applied power to the heaters in a manner that helps drive the measured temperature closer to the desired temperature. This is achieved herein using a PI control scheme.

3. To test the temperature control scheme, enter a desired set point temperature (above room temperature) and then turn on feedback temperature control within the GUI. Observe the measured temperature signal under feedback (closed-loop) control, which is displayed in the GUI for the next few minutes. If the measured temperature of the oil greatly overshoots the desired temperature, reacts too slowly to changes, or fails to converge to the desired set point, the user will need to adjust the control gains to achieve desired closed loop performance.

   NOTE: The program defines a saturation limit for the power (and thus voltage) supplied to the resistive heating elements. For example, two elements reported herein consume up to 5 W power each. Wiring them in parallel means that total power consumption should not exceed 10 W. The user is advised to consider the maximum amount of power that should be supplied to the devices and know that this limit can affect the speed at which the closed-loop system will respond to desired temperature changes. Higher power heating elements enable faster heating and higher set point temperatures but require higher supplied currents for heating.

4. With the system tuned to acceptable closed-loop performance, enter the desired oil temperature for DIB formation as the set point in the GUI.

   NOTE: For example, a set point temperature of 60 °C yielded good results in experiments with BTLE liposomes in the aqueous droplets[37]. The user is referred elsewhere[2,40] for protocols explaining DIB assembly between droplets hanging on wire-type electrodes and configuration of electrophysiology equipment using the patch clamp amplifier, DAQ-1, and electrophysiology measurement software. Specifically, the protocol by Najem, et al.[40] can be closely followed until Step 13. Beyond that step, a slightly different approach is employed for successful monolayer and bilayer formation when using lipids that require heating to promote monolayer or bilayer formation.

5. Lower the tips of the silver/silver chloride (Ag/AgCl) electrodes into the oil until they nearly touch the bottom of the acrylic reservoir. This positioning of the electrode tips is crucial for keeping the droplet on the electrode in heated oil, where convective currents in the oil have been observed to detach droplets from the hydrogel-coated electrodes (**Figure 2c**).

6. Pipette a 250 nL droplet of aqueous lipid solution containing 2 mg/mL of BTLE, 100 mM potassium chloride (KCl), and 10 mM 3-(N-morpholino) propanesulfonic acid (MOPS) onto each electrode tip and let them incubate in the heated oil for a minimum of 10 minutes to promote monolayer formation.

7. Cover the headstage and heated stage fixture with a grounded Faraday cage.

8. Bring the droplets into gentle contact by slowly

manipulating the horizontal positions of the electrodes until the user sees the droplets deform from contact or begin to displace one another and wait a few minutes until bilayer formation commences. If after several minutes a bilayer has not formed, the droplets can be coerced together more to facilitate bilayer formation. The formation of a thinned interfacial bilayer can be confirmed through visual inspection (**Figure 5a**) or by measuring the increase in the amplitude of a square-waveform capacitive current induced by a waveform generator outputting a 10 mV, 10 Hz triangular voltage[22]. Allow the bilayer to equilibrate for a minimum of 10 minutes to reach a steady interfacial area, upon initial formation and prior to subsequent characterization at the initial set point.

NOTE: The type of oil can have a significant impact on bilayer thinning, membrane thickness, and inter-droplet contact angle. In general, the smaller the oil molecule the more easily it can remain in the hydrophobic core of the bilayer occupied by lipid acyl chains. Oil retention increases both monolayer and bilayer tensions and thickness and decreases the area and angle of contact between droplets. These metrics signify a weaker state of adhesion. Larger, bulkier molecules exert the opposite effect. For example, squalene is a bulkier molecule than alkanes such as hexadecane, which enables it to be readily excluded from between monolayers during bilayer thinning. As such, DIBs formed in squalene are thinner, they display higher contact areas and angles, and they exhibit higher free energies of formation[22,42] (a measure of droplet-droplet adhesion).

4. Characterization of temperature-dependent behaviors in DIBs

NOTE: Many physical processes can be studied in DIB-based model membranes, including how changes in temperature affect the structure and transport properties of the membrane. The following steps should be performed after successful bilayer formation at a desired temperature.

1. Measure the nominal capacitance of the membrane while lowering the temperature of the oil bath from a set point that permits bilayer formation to identify thermotropic phase transitions of the lipids in the membrane[38].
    1. Right click the **temperature graph** on the GUI and clear the displayed data. This ensures sufficient space in the buffer is available for subsequent recordings.
    2. Using the waveform generator connected to the patch clamp amplifier, apply a triangular voltage waveform (e.g., 10 mV, 10 Hz) across the DIB electrodes and record the induced current response through the bilayer.
    3. Cool the bilayer by reducing the set point temperature in 5 °C increments and waiting a minimum of 5 min at the new steady state temperature between temperature changes until the desired temperature is achieved. Alternatively, try passively cooling the bilayer by turning off the feedback control system. Be aware, however, that experiments implementing passive cooling from 50-60 °C resulted in higher rates of coalescence.
    4. After the oil bath and bilayer cool to the desired minimum temperature, right click the temperature graph in the GUI again and export the temperature

data versus time to a spreadsheet software. Stop the current recording.

5. From the measured current, calculate the nominal capacitance of the square wave-current response versus time during the cooling period.

6. Plot nominal capacitance (C) versus temperature (T) to observe how membrane capacitance changed. Locate nonmonotonic changes in C versus T to identify T_M.

   NOTE: Nominal capacitance can be calculated from the amplitude of square-wave current[43] ($|I|$) using the relationship $|I| = C\ dv/dt$, where dv/dt is equal to four times the product of the voltage amplitude ($|V|$) and frequency (f) of the applied triangular voltage. From these equations, $C = |I|/(4|V|f)$.

2. Similarly, assess the quasi-static specific capacitance (C_M) of the bilayer at fixed temperatures by successively incrementing the temperature of the oil bath and the bilayer area.

   1. Change the set point temperature in 10 °C increments using the GUI and allow the system to equilibrate to the new temperature.

      1. Perform Step 4.1.2 to initiate the measurement of capacitive current and recording.

      2. Change the bilayer area by carefully adjusting the positions of the electrodes using the micro-manipulators (i.e., separating the electrodes reduces bilayer area). Allow for the square-wave current to reach a steady state amplitude and collect images of the DIB to enable calculation of membrane area versus time by using a camera mounted to the microscope to image the bilayer as seen from the aperture of the microscope stage. Simultaneously, add a digital tag in the current recording software to mark the corresponding timepoint for image collection.

         NOTE: Micro-manipulators allow for the precise control of the electrodes and thus gentle contact between droplets. Coarse manipulation of the droplets can lead to a failed experiment by coalescence of the droplets or by causing a droplet to fall off the electrode. As discussed elsewhere[22], bilayer area is calculated from the contact length between droplets, which appear as overlapping circles in a bottom-view image. The positions and dimensions of the droplets, and the length of the contact line, can be calculated using an image-processing software or with other scientific programming tools.

      3. Repeat Step 4.2.1.2 a minimum of 4 times to obtain a total of 5 DIB images and steady-state regions of bilayer current.

   2. Repeat Step 4.2.1 at each desired temperature.

   3. At the tagged timepoints corresponding to steady-state bilayer areas for acquired images, analyze the current recordings and DIB images to extract C and A data for each temperature.

   4. Plot C versus A data for each temperature and compute the slope of a first-order regression, which represents the C_M of the bilayer at each temperature[22].

   5. Plot values of C_M obtained from Step 4.2.4 versus T.

   6. Examine the C_M versus T data for non-monotonic variations to identify melting temperatures, T_M.

3. Assess the dynamics of voltage-dependent ion channel formation by generating a dc voltage step input across the bilayer.
    1. Set **Initial Voltage** to the desired step value in mV (e.g.,100 mV).
    2. Set **Final Voltage** and **Step Size** to a value higher than the desired step (e.g., 110 mV final voltage and 110 mV step size).
    3. Set a desired duration time for the step input in seconds (e.g., 90 s).
    4. Choose the desired polarity for the step input (e.g., positive).
    5. Switch the patch clamp amplifier to send to the headstage the command voltage originating from the GUI/voltage output module.
    6. Initiate current recordings.
    7. Turn on the voltage and record the induced current response, which should exhibit an S -shaped response to a critical voltage (e.g., ~70 mV for 1 µg/mL Mz in 2 mg/mL BTLE).
4. Separately, dynamic current-voltage relationships for a membrane can be obtained at desired temperatures to reveal voltage-dependent relationships, such as ion channel behaviors.
    1. Switch the patch clamp amplifier to send to the headstage the command voltage originating from the waveform generator and initiate current recordings.
    2. On the waveform generator, output a continuous sinusoidal waveform with a desired amplitude, offset, and frequency.
    3. Record the induced current response across one or multiple cycles.
    4. Repeat as desired for different sine wave amplitudes and frequencies and temperatures.

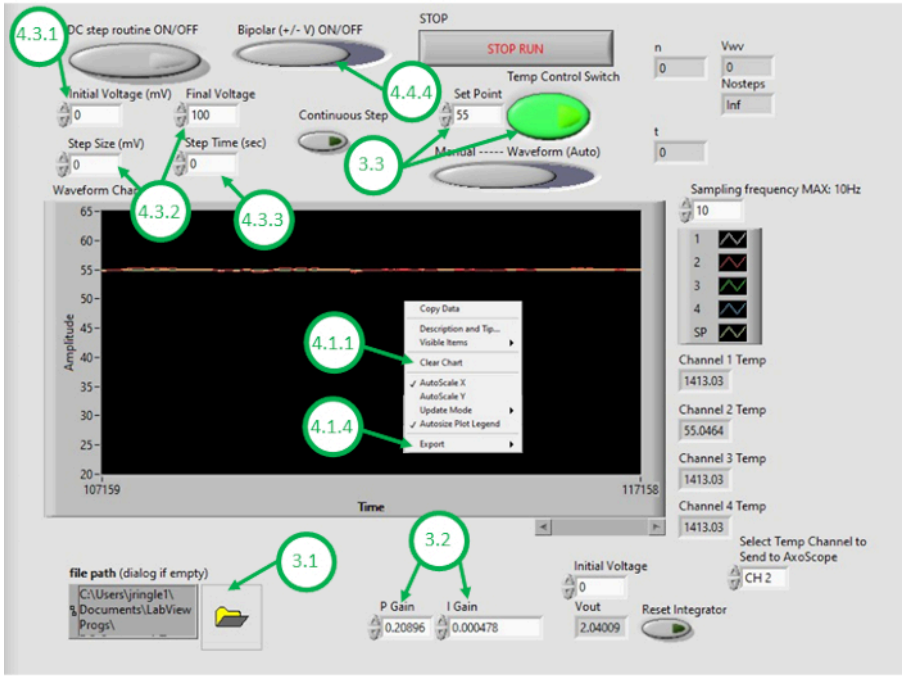

Figure 3: The temperature control GUI. This figure highlights and labels the critical steps required to use the program's GUI to control the temperature of the oil bath. Please click here to view a larger version of this figure.

Representative Results

Figure 1 shows how the aluminum fixture and acrylic oil reservoir are prepared on the microscope stage for DIB formation. Assembly steps 1.2-1.4 serve to thermally insulate the fixture from the stage for more efficient heating. Steps 1.5-1.7 show how to properly attach the thermocouple to the fixture and position the oil reservoir, and steps 1.8 -1.9 show recommended locations for dispensing oil into these pieces.

Figure 2 outlines the components used to establish feedback temperature control and perform electrical measurements on a DIB: a PC, a fixed gain power amplifier, a patch clamp amplifier and a DAQ system (or equivalent instrument for applying voltage and measuring pA-nA level currents), a second DAQ with appropriate analog inputs and outputs, a waveform generator, and the assembled aluminum fixture with attached resistive heaters. DAQ-2 makes use of two modules (**Figure 2b**). A 4-channel, ±10 V, 16-bit analog voltage output module is used to initiate the independent voltages supplied to the input of the power amplifier (blue connection in **Figure 2a**) and an External Command input on the patch clamp amplifier (green connection). The voltage output module is limited by a maximum output current of 46 mA and a maximum output voltage of 10 V, whereas each heating element used herein consumes as much as 5 W of power (~180 mA max) at a maximum voltage of 28 V. For this reason, the power supply/amplifier was included to pre-amplify the output voltage and supplement the supplied current needed for powering the heating elements (wired in parallel) attached to the aluminum fixture. A 4-

channel, 24-bit thermocouple input device is used to digitize temperature measurements from the oil reservoir near the DIB (yellow connection). Since the thermocouple input device module allows up to 4 thermocouples, the user may consider monitoring temperatures at other locations in the fixture. If done, they will also need to consider which signal or combination of signals is used for comparison to the desired set point temperature within the feedback loop.

These outputs and measured signals are controlled via two software: 1) the custom GUI for temperature control; and 2) electrophysiology measurement software. **Figure 3** shows a screenshot of the GUI and includes annotations to corresponding steps in the protocol. The GUI is used to define key parameters (Set Point temperature, PI control gains, voltage limits), compare the measured temperature to the set point temperature and compute the control signal supplied to the amplifier and then the heating elements, and record data of the temperature and applied voltage versus time. This program also includes the ability to command the voltage applied to DIB electrodes (**Figure 2c**) via the patch clamp amplifier. Separately, measurement software is used to configure measurements of both the voltage applied to the DIB electrodes and the induced current through the lipid bilayer. A voltage proportional to DIB current is output by the patch clamp amplifier and sent via BNC cable to DAQ-1 (connection not shown).

Figure 4 plots the change in temperature and absolute electrical power sent to the heaters versus time under both open-loop and closed-loop heating scenarios. For the former, an arbitrary input voltage corresponding to ~5.2 W of power was applied to the heaters, which resulted in an exponential rise in temperature with a time constant of ~125 s and a steady state $\Delta T \approx 4.5$ °C/W after an initial delay of ~20 s. These characteristics of the open-loop system were used to construct a model of the closed-loop system in a simulation software (see **Figure S4** for details) that can be used to determine values for the proportional and integral control gains. The closed-loop and simulated model responses in **Figure 4** thus represent the measured and simulated responses of the tuned PI controller, with K_P and K_I values of 0.598 and 0.00445, respectively, to a set point temperature 20 °C higher than RT. Compared to the open-loop case, both the simulation and the measurements confirm the increased speed of response in the closed-loop system (time constant ~63 s). The reduction in heating time comes at the expense of higher initial applied power. Still, the desired set point temperature and the measured oil temperature remained within 0.6 °C at steady state, which was deemed suitable for use. Total supplied power is limited within the program during closed-loop control so as not to eclipse the 10 W total power limit for the two heaters.

The temperature control system was used to showcase the temperature-dependence of solvent in a DIB formed from BTLE lipids and its impact on membrane capacitance (**Figure 5**). BTLE lipids were chosen for this measurement because heating is required for DIB formation due to a lipid phase transition that occurs between 35-42 °C[38]. The protocol described herein was performed to initiate bilayer formation at 60 °C. Following membrane formation and equilibration, the temperature can be successively lowered or raised as needed to characterize the response of the membrane. For example, **Figure 5a** shows representative measurements of raw capacitive current (square-shaped waveform) and temperature versus time during a heating cycle from RT to ~60 °C. Observe that the amplitude of the capacitive current waveform reduces by more than half as temperature rises, which is caused by the uptake of oil into the hydrophobic

core of the membrane. This change thickens the interface and alters the lateral tension of the bilayer[22,37,38].

The data in **Figure 5b** document changes in *C* (normalized by the capacitance at 27 °C) versus *T* across one complete cooling-heating cycle after initial bilayer formation at 60 °C. Just like in **Figure 5a**, as temperature rises, capacitance drops. However, what this presentation shows more clearly are the nonmonotonic changes that occur at temperatures between ~30-42 °C, which represents the collective melting temperature, T_M, during which the lipid mixture transitions between a liquid-ordered and a liquid-disordered thermotropic phase**.** The temperature where the nonmonotonic change in capacitance occurs corresponds to a change in bilayer thickness from exclusion of oil from the membrane[38]. Also, note that the hysteresis shown between the heating cycle and the cooling cycle is due to irreversible changes in bilayer area that occur between subsequent cycles, which were typically performed 10 min apart.

Similarly, **Figure 6a,b** show how quasi-static measurements of C_m at different temperatures can be used to identify T_M. Here, the area of the membrane is varied successively by manually increasing the distance between the droplet electrodes. During this experiment, the droplets are first pushed together to promote maximum membrane area prior to subsequent reductions in contact area with stepwise separations between the electrodes. At each level of contact, the nominal capacitance of the bilayer is assessed from the induced current and its area is determined through image analysis. Plotting *C* versus *A* allows for a linear regression, where the slope represents the value of C_m as shown in **Figure 6a**. Repeating this procedure across multiple temperatures (**Figure 6b**) shows that C_m decreases by nearly 50% at temperatures above T_M, confirming an increase in the hydrophobic thickness of the membrane due to heating-induced hexadecane uptake (see **Figure S5** for complete *C* versus *A* data). At higher temperatures, the additional solvent in the membrane also reduces the maximum contact area between the droplets, and thus maximum nominal capacitance. Reducing the temperature reverses these effects. The DIB image in **Figure 6c** shows that when the temperature (25 °C) is well below T_M, the membrane can stably adopt a highly adhesive state-even under the tension of stretched droplets caused by well-separated electrodes. This is the result of complete exclusion of hexadecane from the bilayer, which increases the adhesion energy of the droplets. In this state, the bilayer area cannot be reliably changed through manipulation of the electrodes and hinders the ability to accurately measure specific capacitance (see **Figure S5** for more details).

Finally, the representative data in **Figure 7** show how temperature changes can affect the behaviors of pore-forming species that create ion conducting channels through a DIB. Monazomycin (Mz), a positively-charged antibiotic that forms cation selective channels through the bilayer at sufficient transmembrane potentials[37,44], was chosen to demonstrate this relationship. These measurements were conducted on a BTLE-based (2 mg/mL final concentration in both droplets) DIB doped with Mz (1 µg/mL final concentration in both droplets). The current versus voltage traces shown in **Figure 7a** were obtained by applying sinusoidal membrane voltages and measuring the induced current at two different temperatures; the arrows and subsequent numbers in **Figure 7a** aid in visualizing the successive quarters of the sinusoidal voltage with respect to time. This type of measurement is often performed to examine the voltage-dependence of current through ion channels. The data here show that increasing the temperature of the DIB from 27 °C to 45 °C

causes the threshold for channel formation to rise from ~|100 mV| to ~|110 mV|. This change, likely driven by the higher membrane thickness due to absorbed oil, shows that the energy barrier for insertion has risen. The hysteresis in these curves-which signifies memory resistance-can be caused by voltage-induced changes in either bilayer area or the kinetics of Mz channel formation and inactivation[44].

To help separate these factors in DIBs, transient changes in ion current can be measured in response to a DC step voltage. **Figure 7b** shows the measured current density for the same Mz-doped BTLE membrane at the same voltage level (+90 mV) and two different temperatures (27 °C and 45 °C). The data show clearly that the kinetics of the channel responses are quite different. Notably, at 27 °C, the membrane exhibits a faster, larger increase in current that is then followed by a transient decay (the latter is a result of Mz channels translocating across the bilayer to an inactive state[44]). The response is much more muted at 45 °C, where the *S*-shaped rise in current is not proceeded by a subsequent drop. Differences such as these are helpful for assessing the kinetics of channel responses and understanding how these could contribute to the total dynamic resistance of the membrane.

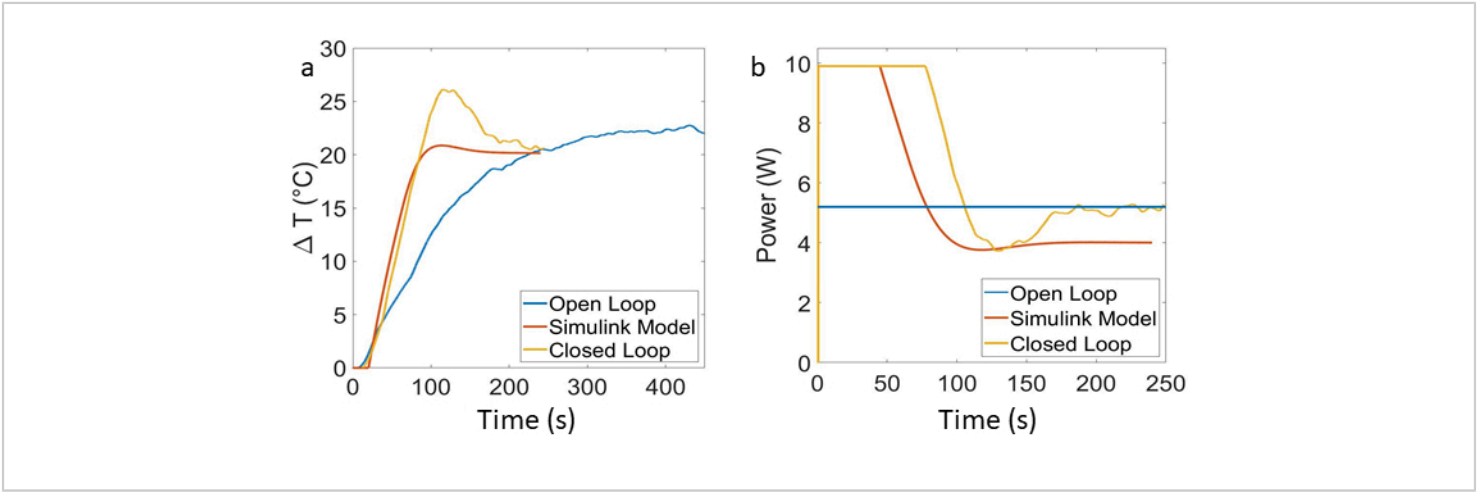

Figure 4: Open-loop versus closed-loop heating. Panel (**a**) compares the time responses for the measured and simulated (See SI) closed-loop system to a +20 °C temperature step to the open-loop heating response under fixed applied power. Panel (**b**) displays the power dissipated by each system. Please click here to view a larger version of this figure.

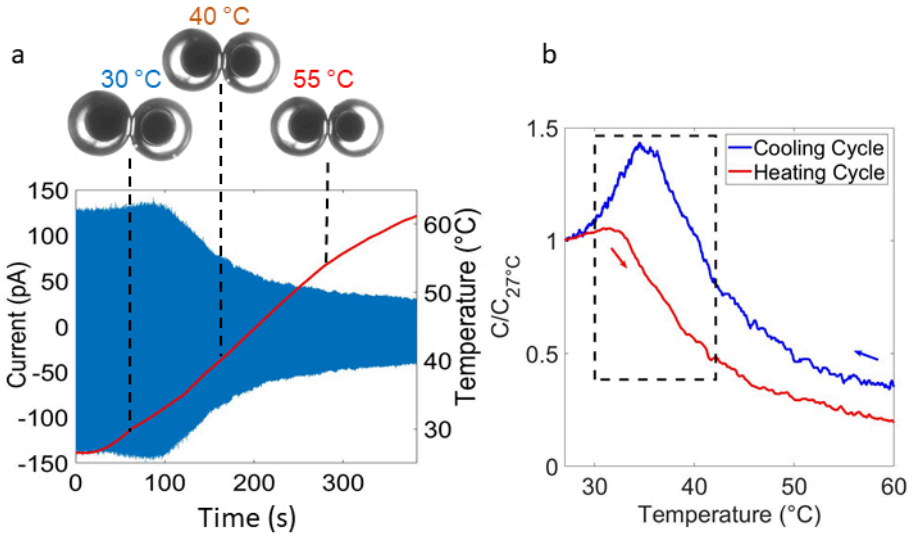

Figure 5: Measuring capacitance and varying temperature. The typical square waveform current response to a 10 mV, 10 Hz triangular waveform input on a BTLE lipid membrane undergoing a phase transition is shown in (**a**). The phase transition of the lipids can also be seen in the area measurement data displayed above panel (**a**). Capacitance normalized by initial capacitance at 27 °C is shown in panel (**b**) plotted as a function of temperature for a heating and cooling cycle. Please click here to view a larger version of this figure.

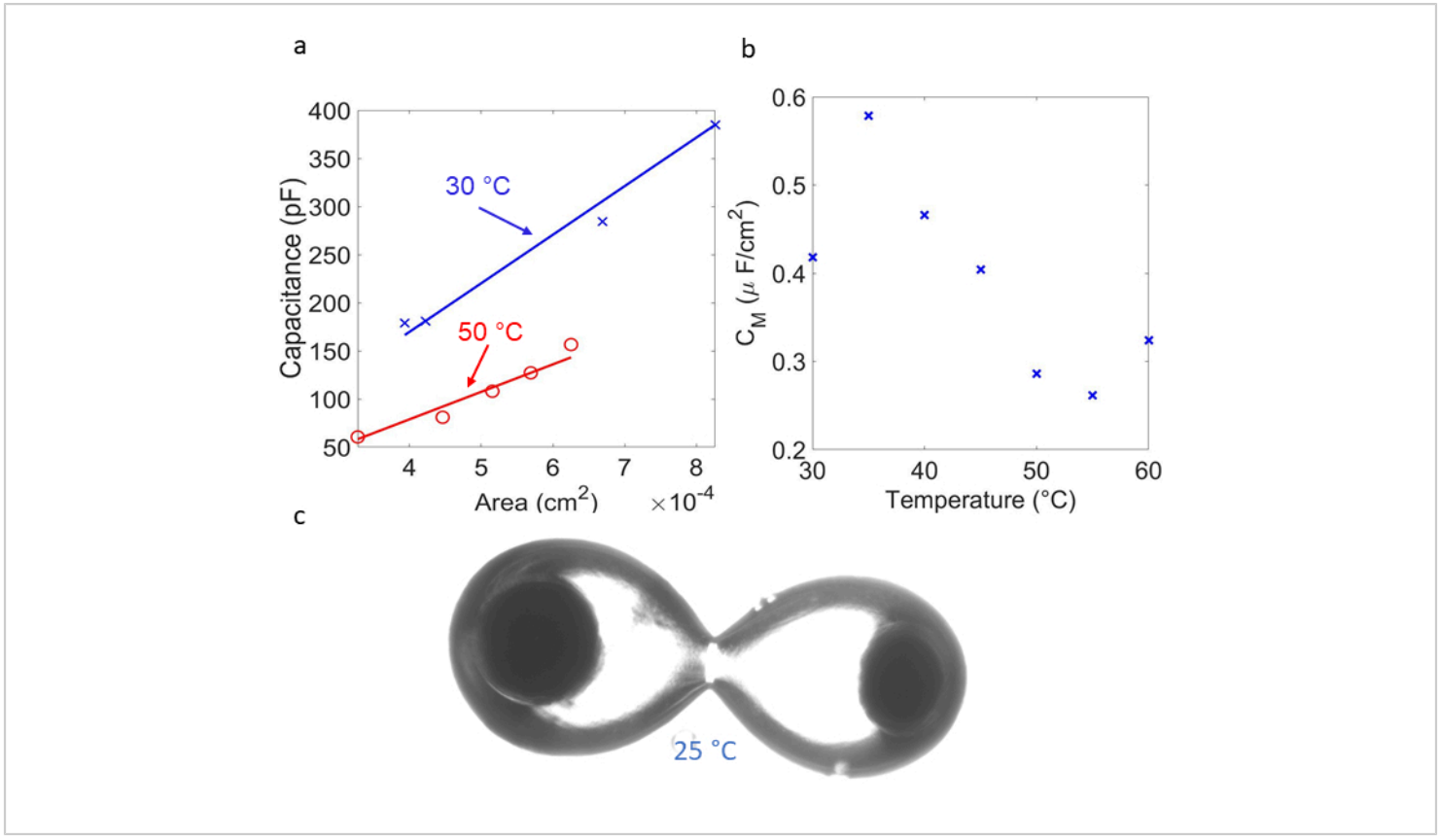

Figure 6: Specific capacitance measurements Panel (**a**) shows nominal capacitance versus bilayer area obtained at successive contact areas for two different temperatures. Linear regressions to each set are used to determine their respective values of C_M. Panel (**b**) plots C_M versus T, while panel (**c**) shows the stable capacitive current waveform (left) and contact area (right) under attempted droplet separation at 25 °C. Please click here to view a larger version of this figure.

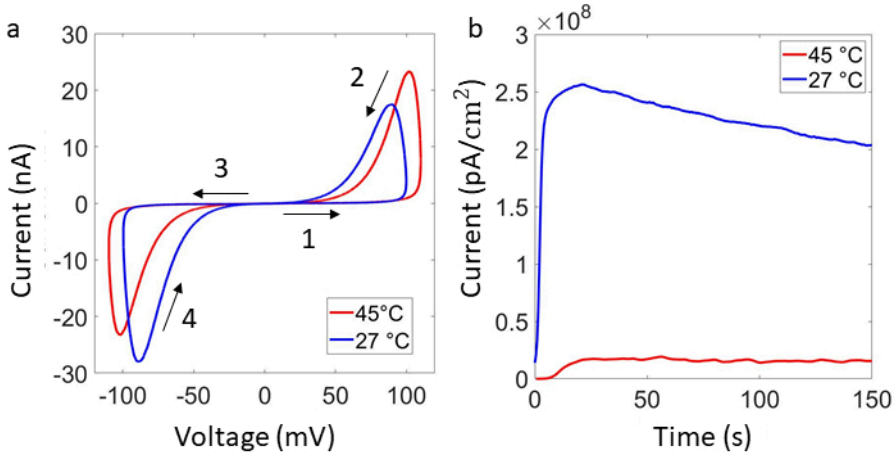

Figure 7: Voltage-dependent membrane resistance and Mz ion-channel kinetics versus temperature. Panel (**a**) shows how the current-voltage relationship changes with temperature for BTLE DIBs formed between droplets containing 1 µg/ml Mz. The arrows and numbers represent the successive portions of the applied sine wave. The differences in these traces illustrate how temperature shifts the voltage threshold for Mz insertion, which is identified as the magnitude of the voltage where induced current increases sharply. Likewise, panel (**b**) shows the impact temperature has on the transient current response induced by a DC step voltage of 90 mV. Please click here to view a larger version of this figure.

Figure S1: Aluminum fixture. This drawing shows the necessary dimensions and features for fabrication of the aluminum fixture that is the base of the heated stage. The 25.2 mm X 26 mm flat spots adjacent to the oil well were designed to allow for a maximal amount of surface-area contact between the fixture and the heating elements for heat conduction. Likewise, aluminum was chosen for the base fixture material due to its high thermal conductivity. The M3 X 0.5 mm screw hole called out in the print is used to secure and position the thermocouple in the oil well. Please click here to download this File.

Figure S2: Acrylic substrate. The acrylic substrate is relatively simple piece to fabricate, with no critical outstanding features, except for the profile. The exterior profile was designed with Poka -yoke in mind so the acrylic substrate can only be oriented in the fixture in such a way to allow ample room for the thermocouple to fit in the oil well. Please click here to download this File.

Figure S3: Heated stage assembly. An exploded view of the assembled heated stage has been provided to aid the experimenter during initial setup. Also, take note of the area highlighted by the dashed circle, as this is the ideal position to fill the aluminum fixture with oil during protocol step 1.8. Please click here to download this File.

Figure S4: Open loop data and Simulink modeling panel. (a) shows the open-loop temperature responses to varying dc power levels that were used to assess the delay time, t_d, the time constant, τ, and open-loop heating gain, α, of the system. The delay time represents the time lag before temperature starts rising (~20 s). Each value of τ (marked by

*, ~125 s) is defined as the time required for 63.2% of the total rise in temperature to occur. Panel (b) shows the steady state change in temperature (ΔT) versus the applied power. The slope of the data plotted in (b) was used to compute the α, which represents the ratio of temperature change per supplied power. These parameters were used in the model shown in panel (c) and provided as a supplementary file to tune the PI controller to achieve a desired closed-loop temperature control response. Please click here to download this File.

Figure S5: Additional specific capacitance data. The plots shown in **Figure 6a,b** were compiled from this C_M data set. This plot also showcases the inability to accurately measure capacitance at temperatures of 25 °C and below, therefore this measurement was excluded from the dataset. The area changes necessary for an accurate C_m measurement require excessive force to be applied to the droplets from the micromanipulators, which causes sever distortion of the droplets shape and area of contact. Please click here to download this File.

Supplementary Coding Files. Please click here to download this File.

Discussion

The protocol described herein provides instructions for assembling and operating an experimental system to control the temperature of the oil and droplets used to form DIBs. It is especially beneficial for enabling DIB formation using lipids that have melting temperatures above RT. Moreover, by precisely varying the temperature of the oil reservoir, the bilayer temperature can be manipulated to study the effects of elevated temperatures on various membrane properties and characteristics, including capacitance, area, thickness, induced thermotropic-phase changes, kinetics of membrane-active species, and the energetics of adhesion of the bilayer interface[37,38].

The protocol consists of three parts prior to use in a DIB study: 1) preparation and assembly of the heated stage fixture; 2) connecting the various instruments; and 3) confirming suitable temperature control performance with the chosen proportional and integral control gains. Most important in part 2, the user must make sure to avoid shared conduction paths between the output of power amplifier (>mA currents) and the patch clamp headstage (pA-nA currents). An inadvertent short could cause permanent damage to the headstage. Additionally, ensuring that the PC and all instruments are connected to a common AC power ground, and the use of a grounded Faraday cage near the headstage and droplet electrodes helps to minimize noise in bilayer current measurements. After setup in part 2 is complete, the user must first assess the open-loop heating response of the oil reservoir by applying a fixed voltage to the heating elements and recording the subsequent rise in temperature (like shown in **Figure 4a**). This type of exponential response can be used to define and simulate a simple model of the closed-loop system for varying values of control gains (see **Figure S4** for details). The control gains reported herein allow the system to heat to a desired temperature level quickly (~ 2 minutes) and with little overshoot and maintain set point value accurately. But the specific gains required will depend on the power level of the heating elements as well as the geometry of the fixture that supports the oil reservoir. Once suitable values of control gains are determined and the feedback control system operates as desired, the user may then begin to assemble and characterize a DIB.

The protocol does not change the process of DIB formation or characterization, however there are limitations and

considerations. Raising the temperature of the oil can affect how droplets hang on the electrodes, due to reductions in monolayer tension and oil density that increase droplet sagging and convective currents in the oil that can move the droplets. Hence, the protocol suggests lowering the tips of the electrodes to near the bottom surface of the substrate such that droplets are supported and held still by the acrylic reservoir. The user should assess how much the substrate may be distorting the droplets (if lowered too far), and consider this distortion when calculating of the area of the bilayer from images of DIBs as discussed elsewhere[22].

While the described system is limited to heating of the oil bath, a Peltier cooling device could be used in place of the resistive heating elements if testing at temperatures below RT is needed. In this case, however, the user will need to consider the freezing point of the oil phase. Many alkanes freeze at temperatures higher that 0 °C; hexadecane described herein freezes at 18 °C. If the oil freezes, droplets will no longer be moveable and a bilayer between droplets may become unstable or rupture.

For a previously untested lipid composition, key unknowns are the incubation time and temperature required to enable sufficient monolayer assembly at the surfaces of the droplets. The general rule is to heat the oil to a temperature above T_M, where lipid mobility is enhanced allowing for faster lateral diffusion and tighter packing at the oil-water interface[45], and wait long enough such that monolayer packing at the oil-water interface is high. The user may review published literature or consider their own complementary measurements to determine suitable time and temperature values: interfacial tension measurements on a pendant drop goniometer can be used to assess the time required for monolayer assembly[46] and differential scanning calorimetry is often used to identify thermotropic transitions of lipids[38]. Or an iterative approach may be pursued to identify suitable time and temperature where bilayer formation is consistent, the membrane is stable for more than a few minutes, and the resistance of the bilayer is >1 GΩ. In recent studies with *E. coli* total lipid extract (ETLE)[37] and BTLE[38,47] a starting temperature >50 °C consistently leads to stable bilayer formation. Similarly, the minimum stable temperature after DIB for a given lipid type may also vary between lipid selections. For example ETLE DIBs can be cooled to 25 °C[37], whereas single component DPPC DIBs always coalesced below T_M~40 °C[38]. Observation has shown that BTLE DIBS show that 27 °C is a safe minimum temperature for maintaining a stable bilayer.

Our representative results show that changes in temperature can greatly affect the properties of the resulting DIB. The data in **Figure 5** shows that the nominal capacitance of the membrane decreases as temperature rises. Because capacitance, *C*, is directly proportional to bilayer area, *A*, and inversely proportional to thickness, *d*, as given by

$$C = \frac{\epsilon A}{d}, \quad (1)$$

a decrease in *C* can be manifest by a decrease in *A*, an increase in *d*, or both (assuming a fixed dielectric permittivity, ε). These relationships motivate the use of capacitance measurements and DIB images to assess changes in *C*, *A*, and C_m versus temperature to determine which effects are significant. The data included in **Figure 5** and **Figure 6** for BTLE DIBs shows that both *C* and C_m (which represents the ratio ε/d) decrease by nearly 50% as temperature rises from 30 C to 60 C. Together, these indicate that higher temperature thickens the bilayer, due to an increased solubility of the acyl chains of the lipids in hexadecane[48]. The additional oil in

the membrane can also affect the interfacial tension of the bilayer and the contact angle between droplets[22,38]. These effects can be quantified by analyzing images of a DIB at user-specified time intervals to monitor bilayer area and contact angle during heating and cooling.

The temperature favorability of oil in the membrane can also be used to assess thermotropic melting temperatures of the lipids and affect ion channel kinetics. The melting temperature for a lipid mixture can be defined by locating nonmonotonic changes in *C* versus *T* relationships as in **Figure 6**. The current measurements in **Figure 7** further reveal that temperature-induced changes in phase (i.e. fluidity) and thickness can impact the threshold voltage for insertion of ionophores like Mz. These physical associations are important for understanding ion channel behaviors in model membranes, especially in scenarios aimed at replicating body temperature environments. However, they may also be useful for tuning the conductivity of the bilayer in applications such as neuromorphic computing devices[47] For example, increased channel kinetics are a desirable feature when fabricating devices exhibiting memory resistance that need to mimic the speed, functionality, and short-term plasticity of the brain.

Disclosures

The authors have no conflicts of interests.

Acknowledgments

Financial support was provided by the National Science Foundation Grant CBET-1752197 and the Air Force Office of Scientific Research Grant FA9550-19-1-0213.

References

1. van Meer, G., de Kroon, A. I. P. M. Lipid map of the mammalian cell. *Journal of Cell Science.* **124** (1), 5-8 (2011).
2. Bayley, H. et al. Droplet interface bilayers. *Molecular BioSystems.* **4** (12), 1191-1208 (2008).
3. Hwang, W. L., Chen, M., Cronin, B., Holden, M. A. Bayley, H. Asymmetric droplet interface bilayers. *Journal of the American Chemical Society.* **130** (18), 5878-5879 (2008).
4. Holden, M. A., Needham, D., Bayley, H. Functional bionetworks from nanoliter water droplets. *Journal of the American Chemical Society.* **129** (27), 8650-8655 (2007).
5. Sarles, S. A., Leo, D. J. Physical encapsulation of droplet interface bilayers for durable, portable biomolecular networks. *Lab on a Chip.* **10** (6), 710-717 (2010).
6. Stanley, C. E. et al. A microfluidic approach for high-throughput droplet interface bilayer (DIB) formation. *Chemical Communications.* **46** (10), 1620-1622 (2010).
7. Gross, L. C. M., Heron, A. J., Baca, S. C., Wallace, M. I. Determining membrane capacitance by dynamic control of droplet interface bilayer area. *Langmuir.* **27** (23), 14335-14342 (2011).
8. Huang, J., Lein, M., Gunderson, C., Holden, M. A. Direct quantitation of peptide-mediated protein transport across a droplet, interface bilayer. *Journal of the American Chemical Society.* **133** (40), 15818-15821 (2011).
9. Leptihn, S., Thompson, J. R., Ellory, J. C., Tucker, S. J., Wallace, M. I. In vitro reconstitution of eukaryotic ion channels using droplet interface bilayers. *Journal of the American Chemical Society.* **133** (24), 9370-9375 (2011).
10. Castell, O. K., Berridge, J., Wallace, M. I. Quantification of membrane protein inhibition by optical ion flux in

a droplet interface bilayer array. *Angewandte Chemie International Edition.* **51** (13), 3134-3138 (2012).

11. Dixit, S. S., Pincus, A., Guo, B., Faris, G. W. Droplet shape analysis and permeability studies in droplet lipid bilayers. *Langmuir.* **28** (19), 7442-7451 (2012).
12. Elani, Y., deMello, A. J., Niu, X., Ces, O. Novel technologies for the formation of 2-D and 3-D droplet interface bilayer networks. *Lab on a Chip.* **12** (18), 3514-3520 (2012).
13. Michalak, Z., Fartash, D., Haque, N., Lee, S. Tunable crystallization via osmosis-driven transport across a droplet interface bilayer. *CrystEngComm.* **14** (23), 7865-7868, (2012).
14. Punnamaraju, S., You, H., Steckl, A. J. Triggered release of molecules across droplet interface bilayer lipid membranes using photopolymerizable lipids. *Langmuir.* **28** (20), 7657-7664 (2012).
15. Boreyko, J. B., Mruetusatorn, P., Sarles, S. A., Retterer, S. T., Collier, C. P. Evaporation-induced buckling and fission of microscale droplet interface bilayers. *Journal of the American Chemical Society.* **135** (15), 5545-5548 (2013).
16. Leptihn, S. et al. Constructing droplet interface bilayers from the contact of aqueous droplets in oil. *Nature Protocols.* **8** (6), 1048-1057 (2013).
17. Villar, G., Graham, A. D., Bayley, H. A Tissue-like printed material. *Science.* **340** (6128), 48-52 (2013).
18. Barriga, H. M. G. et al. Droplet interface bilayer reconstitution and activity measurement of the mechanosensitive channel of large conductance from *Escherichia coli. Journal of The Royal Society Interface.* **11** (98), (2014).
19. Boreyko, J. B., Polizos, G., Datskos, P. G., Sarles, S. A., Collier, C. P. Air-stable droplet interface bilayers on oil-infused surfaces. *Proceedings of the National Academy of Sciences.* **111** (21), 7588-7593 (2014).
20. Mruetusatorn, P. et al. Dynamic morphologies of microscale droplet interface bilayers. *Soft Matter.* 10 (15), 2530-2538 (2014).
21. Najem, J., Dunlap, M., Sukharev, S., Leo, D. J. The gating mechanism of mechanosensitive channels in droplet interface bilayers. *MRS Proceedings.* 1755, Cambridge University Press (2015).
22. Taylor, G. J., Venkatesan, G. A., Collier, C. P., Sarles, S. A. Direct in situ measurement of specific capacitance, monolayer tension, and bilayer tension in a droplet interface bilayer. *Soft Matter.* **11** (38), 7592-7605 (2015).
23. Bayley, H., Cazimoglu, I. Hoskin, C. E. G. Synthetic tissues. *Emerging Topics in Life Sciences.* **3** (5), 615-622 (2019).
24. Oliver, A. E. et al. Protecting, patterning, and scaffolding supported lipid membranes using carbohydrate glasses. *Lab on a Chip.* **8** (6), 892-897 (2008).
25. Maglia, G. et al. Droplet networks with incorporated protein diodes show collective properties. *Nature Nanotechnology.* **4** (7), 437-440 (2009).
26. Najem, J. S. et al. Activation of bacterial channel MscL in mechanically stimulated droplet interface bilayers. *Scientific Reports.* **5**, 13726 (2015).
27. Freeman, E. C., Najem, J. S., Sukharev, S., Philen, M. K., Leo, D. J. The mechanoelectrical response of droplet interface bilayer membranes. *Soft Matter.* **12** (12), 3021-3031 (2016).

28. Tamaddoni, N., Sarles, S. A. Toward cell-inspired materials that feel: measurements and modeling of mechanotransduction in droplet-based, multi-membrane arrays. *Bioinspiration & Biomimetics.* **11** (3), 036008 (2016).
29. Restrepo Schild, V. et al. Light-patterned current generation in a droplet bilayer array. *Scientific Reports.* **7**, 46585 (2017).
30. Milianta, P. J., Muzzio, M., Denver, J., Cawley, G., Lee, S. Water permeability across symmetric and asymmetric droplet interface bilayers: Interaction of cholesterol sulfate with DPhPC. *Langmuir.* **31** (44), 12187-12196 (2015).
31. Mruetusatorn, P. et al. Control of membrane permeability in air-stable droplet interface bilayers. *Langmuir.* **31** (14), 4224-4231 (2015).
32. Wauer, T. et al. Construction and manipulation of functional three-dimensional droplet networks. *ACS Nano.* **8** (1), 771-779 (2013).
33. Bayley, H. Building blocks for cells and tissues: Beyond a game. *Emerging Topics in Life Sciences.* **3** (5), 433-434 (2019).
34. Booth, M., Restrepo Schild, V., Downs, F. Bayley, J. Droplet network, from lipid bilayer to synthetic tissues. in *Encyclopedia of Biophysics.* Springer. (2019).
35. Booth, M. J., Cazimoglu, I., Bayley, H. Controlled deprotection and release of a small molecule from a compartmented synthetic tissue module. *Communications Chemistry.* **2** (1), 142, (2019).
36. Gobbo, P. et al. Programmed assembly of synthetic protocells into thermoresponsive prototissues. *Nature Materials.* **17** (12), 1145-1153 (2018).
37. Taylor, G. J., Sarles, S. A. Heating-enabled formation of droplet interface bilayers using escherichia coli total lipid extract. *Langmuir.* **31** (1), 325-337 (2015).
38. Taylor, G. J. et al. Capacitive detection of low-enthalpy, higher-order phase transitions in synthetic and natural composition lipid membranes. *Langmuir.* **33** (38), 10016-10026 (2017).
39. Lee, S., Kim, D. H., Needham, D. Equilibrium and dynamic interfacial tension measurements at microscopic interfaces using a micropipet technique. 2. Dynamics of phospholipid monolayer formation and equilibrium tensions at the water-air interface. *Langmuir.* **17** (18), 5544-5550 (2001).
40. Najem, J. S. et al. Assembly and characterization of biomolecular memristors consisting of ion channel-doped lipid membranes. *Journal of Visualized Experiments.* (145), e58998 (2019).
41. Wang, Y.-G., Shao, H.-H. Optimal tuning for PI controller. *Automatica.* **36** (1), 147-152 (2000).
42. Needham, D., Haydon, D. A. Tensions and free energies of formation of "solventless" lipid bilayers. Measurement of high contact angles. *Biophysical Journal.* **41** (3), 251-257 (1983).
43. Sarles, S. A., Leo, D. J. Physical Encapsulation of Interface Bilayers for durable portable biolayer network. *Lab on a Chip.* **10** (6), 710-717 (2010).
44. Muller, R. U., Peskin, C. S. The kinetics of monazomycin-induced voltage-dependent conductance. II. Theory and a demonstration of a form of memory. *The Journal of General Physiology.* **78** (2), 201-229 (1981).

45. Nenninger, A. et al. Independent mobility of proteins and lipids in the plasma membrane of *Escherichia coli. Molecular Microbiology.* **92** (5), 1142-1153 (2014).

46. Venkatesan, G. A. et al. Adsorption kinetics dictate monolayer self-assembly for both lipid-in and lipid-out approaches to droplet interface bilayer formation. *Langmuir.* **31** (47), 12883-12893 (2015).

47. Najem, J. S. et al. Memristive ion channel-doped biomembranes as synaptic mimics. *ACS Nano.* **12** (5), 4702-4711 (2018).

48. Tamaddoni, N., Taylor, G., Hepburn, T., Michael Kilbey, S., Sarles, S. A. Reversible, voltage-activated formation of biomimetic membranes between triblock copolymer-coated aqueous droplets in good solvents. *Soft Matter.* **12**, 5096 - 5109 (2016).